A Comparison of Three Methods for the Quantification of Greenhouse Gas Emissions from Spontaneous Combustion in Open-Cut Coal Mines

William Lilley, Stuart Day, David Williams and John Carras,

CSIRO Energy Technology

PO Box 330 Newcastle NSW 2300, Australia

Phone: 61 2 4960 6000

Fax: 61 2 4960 6054

Email: william.lilley@csiro.au

Abstract

Greenhouse gas emissions from spontaneous combustion in coal mines are currently not included by the Inter-Governmental Panel for Climate Change (IPCC) in national greenhouse gas inventories because there are no robust methods available to quantify the emissions. This paper reports on investigations of three approaches being pursued to provide sufficiently robust methods to enable these emissions to be included in inventories. The first method was based on the use of airborne thermal infrared photography coupled with chamber measurements of emissions from hot mine spoil pile surfaces. In the second method, downwind plume geometry and crosswind traverses of the plume using an instrumented vehicle were used to estimate the emission flux from spontaneous combustion. The third method was based on inverse atmospheric modelling using stationary CO_2 monitors.

All three methods showed considerable scatter in the estimates produced but also showed significant overlap. While the three methods used in this study have shown convergence, there is still considerable uncertainty associated with any single approach.

Keywords: coal mining, greenhouse, spontaneous combustion, inverse modelling, remote sensing

1 *Introduction*

Spoil piles in surface (open-cut) coal mines are formed as a necessary part of the mining process since overburden must be removed to expose the underlying coal seams. Overburden often consists of inert materials, but it may also contain significant quantities of carbonaceous materials including carbon-containing shales, low quality coal or thin and uneconomic coal seams. It is common practice for these carbonaceous materials to be dumped and become part of the spoil pile.

In Australia, mining licences generally require the spoil piles to be rehabilitated and the land returned to its pre-mining use, however, in some circumstances spontaneous combustion may develop before, or even after, the rehabilitation has been completed. This can present a major issue for the coal mining companies and regulatory authorities.

Self-heating in coal is the result of the exothermic reaction of coal with oxygen from the atmosphere. The heat, if it accumulates, causes a temperature rise that

accelerates the rate of oxidation and heat release, which if unchecked, may result in spontaneous combustion. Spontaneous combustion is a relatively common phenomenon in the coal industry and has been the subject of research for many years; see Glasser and Bradshaw (1990), Carras and Young (1994), Walker (1999), and Nelson and Chen (2007) for reviews. In underground coal mines its occurrence has often led to the loss of life, particularly when it occurs in mines with high methane contents that can produce explosive atmospheres. Indeed, most of the work that has occurred worldwide has focussed on empirical methods for predicting or controlling spontaneous combustion in underground mines. In open-cut coal mines spontaneous combustion has often been seen as less important but this perception is changing with pressure coming from two major sources. One concerns emissions of air pollutants such as SO_2, NO_x, fine particles and air toxics (Finkelman, 2004; Stracher and Taylor, 2004). The other relates to the increasing international pressure to curb greenhouse gas emissions.

Spontaneous combustion in spoil piles in open-cut coal mines has been recognised by the Inter-Governmental Panel for Climate Change (IPCC) as a potential source of greenhouse gas emissions (IPCC, 2007). However, it has been excluded from greenhouse gas inventories as it is considered that there is no acceptable routine method for estimating the emissions from spontaneous combustion. There are two main reasons for the lack of a suitable method. One of these results from the fact that due to the large areas involved, even small emission rates can't be ignored as the integrated emissions across the large area with small emissions per unit area, may make a very significant contribution to the total emissions.

Carras et al. (2009) recently reported the use of a flux chamber method to estimate emissions from spontaneous combustion in open-cut coal mines. Measurements of emissions from spoil piles, coal rejects and tailings were conducted at 11 mines in Australia using the chamber technique. These authors measured emission rates, in CO_2 equivalent (CO_2-e) ranging from 12 kg CO_2-e yr^{-1} m^{-2} to 8200 kg CO_2-e yr^{-1} m^{-2}, depending on the severity of the spontaneous combustion. While that study provided the first direct measurement of greenhouse gas emissions from spontaneous combustion and low temperature oxidation, the methodology was found to be extremely labour intensive and limited in its spatial and temporal resolution.

As a result of these limitations we have pursued other methods to estimate emissions from spontaneous combustion and these are the focus of the work reported here

2 *Experimental Methods*

A brief description of the three methods developed to estimate the emissions from spontaneous combustion follows. The three methods were:

1. The chamber method reported by Carras et al (2009) coupled to airborne infrared thermography which provided an extended map of elevated surface temperature due to spontaneous combustion,
2. A method based on downwind plume geometry and the physics of plume dispersion in the atmosphere and,
3. Inverse atmospheric modelling also based on the physics of plume dispersion in the atmosphere but using stationary CO_2 monitors and long term observations.

All three methods were applied to a region in the Hunter Valley in New South Wales (NSW) where there was active and widespread spontaneous combustion in spoil piles. The inverse modelling method was also applied to a mine with spontaneous combustion in the Bowen Basin region in Queensland.

2.1 Airborne infrared thermography

Carras et al. (2009) reported an approximate correlation between the emissions measured by a flux chamber and the surface temperature of the area of spoil where the measurements were made. Their data are summarised in Figure 1.

Figure 1

This correlation, when coupled with a map of a spoil pile that shows surface temperature and area, provides a way to estimate spontaneous combustion emissions.

Infrared data were obtained by Air Target Services Pty Ltd using a Daedalus 1268 Airborne Thematic Mapper (ATM) system fitted to a Cessna 414A aircraft. The Daedalus instrument is capable of sensing 12 individual wavelength bands from ultraviolet to infrared however, for this work, only the infrared bands were used. Two sets of data in the wavelength range of 8-14 μm were obtained during the flight.

A flight was made during October 2001, covering an area of approximately 12 × 8 km in the Hunter Valley to include the target mines. The aircraft flew at an altitude of approximately 1000 m, producing thermal images of the ground showing detail down to about 2 m. Each pass of the aircraft yielded a swath of data between about 1200 and 1600 m wide. To avoid the effects of solar heating of the ground surface and to maximise thermal contrast, the flight was made before dawn under cloudless and windless conditions.

Data representing surface temperature were recorded as pixels at 8-bit integer resolution. The instrument was set to provide two bands of data with different gains so that high temperature regions did not saturate the detector. Ground level measurements of distinctive surface features (eg water storage dams, roads and natural ground) were also made at the same time as the flight to provide calibration for the infrared data.

The swaths were analysed using ArcGIS software to provide a thermal representation of the region which was then divided into a grid of 100 × 102 cells each 50 x 50 m in size. Figure 2 shows the thermal image for the region studied in this work where elevated temperatures are indicated by light coloured pixels, and clearly show the extensive heating in the spoil at the time of the flight.

Insert Figure 2

In Figure 2 the ambient temperature of unaffected ground (eg the dam in the upper left hand corner) was approximately 10 °C at the time of measurement.

Using the linear relationship shown by the line in Figure 1, a mean emission rate was calculated for each cell having a mean temperature of 10 °C (i.e. the ambient temperature of the ground at the time of the flight) or higher.

Areas of the ground surface that did not contribute to greenhouse emissions (such as water storage dams) were arbitrarily set to 0 °C so as not to be counted in emissions calculations.

Total emissions for the affected area were calculated by summing the emissions for each grid cell.

2.2 Plume traverses

Direct measurements of the ground level CO_2 concentration within the plume were made by traversing a vehicle fitted with an infrared CO_2 analyser (Ecotech Model ML9820) travelling through the plume at about 20 km hr^{-1} downwind of the source. The two dashed straight lines in Figure 2 show the path traversed in order to intersect the plume. The position of the vehicle was monitored continuously using a GPS receiver. Data from the gas analyser and GPS were logged at 1 Hz on a laptop computer. Information on the vertical extent and structure of the plume was obtained from a combination of local meteorological data (wind speed and direction measured at 10 m above ground level) and plume modelling using the air quality model, TAPM (Hurley, 2005) that has been widely used in previous air quality modelling studies (e.g. Luhar and Hurley, 2003; Zawar-Reza et al., 2005).

The average concentration of a plume traverse was used to estimate the area wide flux by:

$$Q_i = u \int_{-y'}^{+y'} \int_{0}^{z_i} c(x,y,z)dydz \qquad (1)$$

where c is the average cross wind concentration, u is the average wind speed over the plume extent, Q_i is the average emission rate for the period of measurement, and $-y'$, $+y'$ and z_i are the plume dimensions in the crosswind and vertical directions, respectively.

The vertical extent of the plume, z_i, was modelled using TAPM. As measurements were taken sufficiently close to the emission site that the plume could not be assumed to be uniformly mixed at the point of measurement, a scaling factor, α, based on the vertical spread of the plume as predicted by TAPM was used to estimate the vertical averaged concentration, c, by adjusting the measured ground level concentration, c_g. The scaling factor, α, is given by

$$\alpha = \frac{\int_{0}^{z_i} c dz}{\int_{0}^{10} c_g dz} \qquad (2)$$

where c_g is the average concentration output for bottom most layer from the TAPM model which represents a layer between the ground and 10m in height. For current purposes this has been taken to be the same as the ground level concentration.

Plume traverses were made around the perimeter of the mine when prevailing wind conditions were likely to drive the plume across accessible roads.

2.3 Inverse modelling technique

The approach taken here is based on a modification of the earlier work of Lehning et al. (1994) who developed an inverse technique for determining area source emissions from measured downwind concentrations. Lehning et al. used two receptor arrays positioned downwind of the source. Their model treated dispersive processes with a Gaussian assumption for horizontal diffusion and either a Gaussian or Huang (Huang, 1979) similarity solution for dispersion in the vertical direction. They found that by using two arrays they were able to reconstruct the spatial pattern of an emission source, measuring 20 m × 20 m in size, by taking measurements at 11 locations in each array.

Briefly, the degree of dispersion from an area source at the receptor can be written:

$$c(x,y,z) = \int_{-x_s}^{+x_s} \int_{-y_s}^{+y_s} Q'(x',y')K(x,y,z,x',y')dx'dy' \quad (3)$$

where Q' is the source flux, c is the concentration at position x,y,z (where z represents the height above ground, and x and y are the locations of the downwind and crosswind boundaries of the source area), and x' and y' are the coordinates of the source area.

By dividing the source into a number of unit cells, Equation 3 becomes:

$$c(x_j,y_j,z_j) = \sum_{x_i}\sum_{y_i} Q'(x_i,y_i)K(x_j,y_j,z_j,x_i,y_i)\Delta x_i \Delta y_i \quad (4)$$

where the subscripts i and j represent the source and receptor locations respectively.

The formulation used for the kernel (K) in the current study is based upon the Gaussian equation, and for a ground level source is given by

$$K(x_j,y_j,z_j,x_i,y_i) = \frac{1}{\pi\sigma_y\sigma_z u}\exp\left(-\frac{(y_j-y_i)^2}{2\sigma_y^{\,2}}\right) \quad (5)$$

where u is the wind speed, σ_y and σ_z are the horizontal and vertical dispersion coefficients derived from a Pasquill Gifford scheme determined from the distance of the source to the receptor, x_j,y_j,z_j represents the receptor location, and x_i,y_i represents the location of the source.

Lehning et al. (1994) also developed an iterative process to drive the equations to a stable solution. This method uses an initial seed value for each grid cell and then calculates residuals from the deviation between the calculated receptor concentration, c_{calc}, at each iteration and the measured data set c_{obs}:

$$res(x_j,y_j,z_j) = res_j = \frac{c_{obs}(x_j,y_j,z_j) - c_{calc}(x_j,y_j,z_j)}{c_{obs}(x_j,y_j,z_j) + c_{calc}(x_j,y_j,z_j)} \quad (6)$$

The calculated emission flux for each cell is then adjusted with the correction factors, f_i, to give the new emission fluxes, Q_i, and then repeated until the residual becomes sufficiently small (i.e. $<10^{-3}$).

$$f_i = \prod_j \left(1 + \frac{Fres_j K_{ij}}{\sum_j K_{ij}}\right) \quad (7)$$

$$Q_i^{new} = f_i Q_i^{old} \quad (8)$$

where F is a factor used to decrease the number of iterations. (Complete details of the iteration procedure can be found in Lehning et al., 1994).

In the current work, the method of Lehning et al. (1994) has been adapted to use data measured at either one or two locations. In these cases, the method works by using observations from multiple wind directions resulting in a series to which the iteration method can be applied. This series can be considered analogous to a version in which observations for two wind directions are taken at points distributed in two arcs surrounding the source.

In the Hunter Valley of NSW only one monitor could be deployed due to restricted access to private land and limited availability of power to the site. Consequently only one monitoring site was used. A single fixed CO_2 monitor (Ecotech Model ML9820)

was placed in a building in the south-east corner of the region as shown in Figure 2 and logged data continuously over approximately a six-month period. Meteorological data, including wind speed and direction, were measured as 15-minute averages at a site approximately 2 km from the monitor.

For the Bowen Basin mine two monitors (Ecotech Model ML9820) were used as shown in Figure 3.

Insert Figure 3

Meteorological data were obtained from a monitoring station located with one of the gas monitoring locations.

To form a sampling array for use in the model, data from the CO_2 monitors were sorted into blocks of 5° wind direction increments for which an average wind speed and concentration was determined from local wind speed data and ground level measurements. Averaging of concentrations and wind speed into these well defined divisions results in a smoothing of small differences in dispersive processes for similar atmospheric conditions and for temporal changes in emission rates. Data for wind speeds less than 0.5 m s^{-1} were filtered out. Emission estimates were derived for neutral and slightly stable meteorological conditions (i.e. Pasquill Gifford classes D and E) as these conditions were found most conducive for capturing elevated concentrations by the CO_2 monitors employed in this study.

When using the Gaussian formulation it is possible for the method to give rise to artefacts due to small kernel values. To minimise this effect, the model was operated by capping the maximum emission flux in each cell. An iterative procedure was adopted by setting the maximum flux at a low value and operating the model with incremental increases in the capped value. The model was repeatedly run until the solution converged and little change was apparent with increasing the maximum cell flux.

Seed values for the inverse modelling for the Hunter Valley were obtained from Figure 2 by superimposing a 50 X 50 m grid covering a total area of 5 km × 5 km. The grid was initialised by using seed values based on the emissions distribution calculated from the thermal imagery. All other areas were assigned zero emissions.

Thermal imagery was not available for the Bowen Basin mine so the model was initialised with simple seed values based on the advice of mine site personnel who were able to identify areas of significant spontaneous combustion activity. Figure 3 displays the emissions grid used to initialise the inverse model. The areas designated as prone to self heating (red) were set with the largest seed value while general disturbed mine site areas (yellow) and rehabilitation zones (green) were set with a small seed value.

3 *Results*

3.1 Averaging times

Each of the three methods developed to determine greenhouse gas emissions from spontaneous combustion has its own characteristic averaging time. For instance the infrared method determined surface temperatures over a period of ~10 minutes. Also, the plume traverse method sampled the downwind plume over a period of ~30 minutes. The inverse method provided information over the timeframe for which data were accumulated, which was typically of order of three to six months. Consequently the first two methods provide somewhat 'instantaneous' values compared with the

longer time average of the third method. Developing annual emission rates from short term measurements is an important consideration that will be discussed later in this work.

3.2 Emission estimates from thermal imagery

In Figure 4, the area of the ground above 10 °C is plotted as a function of the average surface temperature of each 50 × 50 m cell determined from the thermal imagery. An interesting feature of this plot is that even though surface temperatures measured in cracks on some parts of the spoil were found to be in excess of 400 °C, the total area of these very hot regions represented only a very small fraction of the total area of a 50 x 50 m cell. The result of this is that the 50 x 50 m area average temperatures are much smaller than the peak values and this is shown in Figure 4 where more than 90 % of the area showing signs of heating was less than 20 °C.

Figure 4

Applying the relationship shown in Figure 1 to the thermography in Figure 2 yielded a total emission flux for the area of 76 kg CO_2-e s^{-1}. Note that because of the temperature distribution shown in Figure 4, most of the emissions were associated with the low temperature areas.

While this method has certain advantages for measuring emissions from spontaneous combustion (it can be used to cover wide areas quickly) there are several factors that influence the uncertainty associated with the emission estimates. One of the key considerations is the accuracy of the ground temperatures derived from infrared data. The ground temperature is not directly measured but rather calculated from the radiation detected by the sensor in the aircraft and also the emissivity of the reflective surfaces. Since the emissivities of natural surfaces are known to vary, without detailed knowledge of the surface there may be a significant error in the calculated temperature. We estimate that the uncertainty in the surface temperature inferred from the thermography data is at least ± 3 °C (Day et al., 2010). Since the bulk of the emissions are derived from low temperature heating, the temperature below which emissions are assumed to be zero can strongly affect the emission estimate. To illustrate the sensitivity of the method to this "threshold" temperature, we recalculated the emissions using 15 °C rather than 10 °C used previously. In this case the annual emission estimate was halved, reducing to 40 kg CO_2-e s^{-1}.

3.2 Plume Traverses

Plume traversing is opportunistic because it can only be carried out in favourable weather conditions and also relies on being able to access the plume. Consequently, it is difficult and time consuming to obtain large data sets. In this study, six successful plume traverses were made along the two roadways shown by straight lines in Figure 2 over a period of about 6 months. Due to the remote location of the Bowen Basin site, it was not practical to conduct traverses at that site.

An example of the traverse results for the Hunter Valley is shown in Figure 5 where the ground level CO_2 concentration (above background) measured during two consecutive traverses along the southern roadway indicated in Figure 2 is plotted as a function of the vehicle position.

Figure 5

The traverses show the large horizontal extent of the plume (~5 km), confirming the wide distribution of spontaneous combustion within the region (as shown in the thermal image in Figure 2).

Table 1 shows a summary of the results from each of the 6 traverses that were successfully carried out. (Note Table 1 also shows the data for all three methods used in the Hunter Valley, for completeness). The first four sets of data ranged in value between ~26 to 51 kg CO_2-e s^{-1}. The final two values were significantly higher at 117 and 178 kg CO_2-e s^{-1}. While it is not immediately apparent why there is such a large difference between the data from the first four traverses and the final two the weather conditions prevailing at the time of measurement were very different. The first four traverses were carried out during winter conditions with typically low wind speeds (< 1ms^{-1} on three occasions and < 4 ms^{-1} for one traverse) and calm conditions and ambient temperatures <18°C. The last two traverses were carried out during summer under gusty conditions with an average wind speed of about 5 m s^{-1} and the ambient temperature ~40°C. It is possible that the hotter gustier conditions may have been fanning the combustion leading to increased emission rates.

3.3 Inverse calculations

Results for the Hunter Valley are presented in Figure 6. The model results are for D class stability (neutral, Figure 6a) or E class stability (slightly stable conditions, Figure 6b). For comparison, the emissions calculated using the infrared imagery are also shown (Figure 6c) and these values were used as seed values for the inverse modelling.

Insert Figure 6

The estimated total CO_2 emission flux for the region from the inverse model ranged from 33 to 51 kg CO_2-e s^{-1} for stability classes E and D respectively

In Figure 7 the CO_2 flux calculated for the Bowen Basin mine is shown. Figures 7a and 7b correspond to the flux estimates for stability classes D and E respectively, and Figure 7c shows the initialising grid used at this site.

Insert Figure 7

Table 2 shows the calculated emission rates for the Bowen Basin data. The Bowen Basin mine site contained two monitors, but only a relatively small amount of data were available for modelling purposes. This was due to the dispersed pockets of self-heating within the mine so that in many cases, emissions were not passing over the monitors. On some occasions when elevated CO_2 concentrations were detected, the very low wind speeds prevailing precluded the use of the data in the model. Nevertheless, there were sufficient data to be able to detect the areas of spontaneous combustion in the mine that had been previously recognised by mine staff.

In addition to these outbreaks, the model also found a number of other sources of elevated emissions in coal stockpiles elsewhere on the mine site. Subsequent discussions with mine staff confirmed that these areas could be prone to self-heating although they were considered less significant than other areas within the mine.

The range of fluxes estimated for the Bowen Basin mine was 6 to 10 kg CO_2-e s^{-1} for stability classes E and D respectively.

4 Discussion

The data in Table 1 show the emissions rates for all three methods expressed as mass per second and also annualised to units of mass per year simply by multiplying by the number of seconds in the year. While this is a reasonable approach for the longer averaging time data from the inverse modelling, the data from the traverses in particular is more problematic. Given the limited data available and if there is a meteorological dependence of the emission rates as discussed above then significantly more traverse data would be required to present an annually weighted emission. In the current work such data are not available, however, we note that an examination of historic meteorological data for Singleton, which is near the measurement site, shows that, there are typically less than 3 days per year when the temperature is over 40 °C and the wind speed is over 5 ms^{-1} (Aust. Gov. Bureau of Meteorology, 2010).

The ranges of the emissions determined for both the Hunter Valley and Bowen Basin sites are shown in Figure 8 on an annualised basis.

Figure 8

For the Hunter Valley, the results for the three methods exhibit a considerable range, but the estimates are broadly consistent. (Note we have restricted the data from the traverse method to the first four traverses for the reasons described above, but have indicated the uncertainty on the upper bound by use of the dashed line).

Emissions from the Bowen Basin mine were much lower than for the region in the Hunter Valley, despite both regions having histories of spontaneous combustion in the spoil piles. It appears that in the Bowen Basin mine, the affected areas are localised and geographically sparse compared to the Hunter Valley site.

When interpreting the above results it is important to consider the uncertainties associated with each method.

For the thermal imagery one of the largest sources of uncertainty is the method's dependence on an accurate knowledge of the ground temperature. As has already been discussed, the temperature values returned by the method may have significant errors if the emissivity of the ground surface is not known. This in turn affects the threshold temperature (i.e. the temperature below which emissions are assumed to be zero), which as shown previously , is a strong determinant of the magnitude of the final emission estimate. It is crucial that the thermal data be obtained under ambient conditions similar to those prevailing when the temperature/emission data (Figure 1) were obtained. If, for example, the infrared survey was flown during the summer months, the temperature of the unaffected ground would have been substantially higher and using the data in Figure 1 would have overestimated the emission flux. Conversely if the ground temperature was less than 10 °C, the estimate would have been too low.

Another source of error associated with estimating emissions fluxes from infrared data is apparent from the degree of scatter in the relationship between emission flux and temperature shown in Figure 1. While the data in Figure 1 show a clear relationship between emission rate and temperature there is a large degree of inherent scatter around the line of best fit to the data. The scatter arises principally from two sources;

1. The surface temperature is a function of the intensity of heating beneath the surface, the nature of the surface, the location of the heating relative to the surface and the intervening thermal properties and the meteorology at the time the measurements were made.
2. The emission rate depends on the intensity of the heating as well as on the structure of the ground between the surface and the location of the heating i.e. cracks and channels will provide higher permeability pathways for gas flow than will compacted soil or clay.

Further measurements to better define this relationship may reduce the scatter somewhat, but high levels of variability are inevitable given the inhomogeneous nature of spoil piles.

In the plume traversing method, the largest uncertainty resides in determining the plume characteristics. In this study, we measured the concentration at ground level and the plume characteristics were modelled using TAPM, a model that predicted local meteorological conditions and the plume geometry. This will also be introducing uncertainty into the calculations as the model output may not be reflecting accurately the specific features of the days when the measurements were made. The calculated emission flux depends on the exact CO_2 concentration across the entire cross section, the vertical extent of the plume where the measurements were taken, the local micrometeorology including wind speed and especially the local atmospheric stability. These factors are all part of the stochastic nature of the atmospheric boundary layer and are subject to considerable uncertainty for an "instantaneous" traverse.

The traverse results in Table 1 show that there is substantial variation in the emission fluxes with the two traverse made during summer conditions being significantly greater than the traverse in the winter. If this is generally the case for spontaneous combustion in spoil piles then it is evident that single measurements will not accurately reflect the true annual emissions. Consequently, to obtain reliable emission estimates using this method, it would be necessary to conduct numerous traverses throughout the entire year

For the inverse methods the uncertainties are also mainly related to the ability of the model to accurately predict downwind concentrations of CO_2 for extended periods and, potentially, intermittent sources. The method also requires a considerable degree of data filtering. In our study, readings made in wind speeds of less than 0.5 m s^{-1} were discarded to ensure that the model performed well. Other studies using inverse techniques to measure wide-area emissions have also noted the requirement for rigorous data filtering (Loh et al., 2009). The consequence of data filtering is that it reduces the available data, and hence the robustness of the estimate.

While the inverse model shows promise as a technique for evaluating area wide fluxes, in the current application where the number of monitors was far from optimum the method relies to a large extent on a reasonable seed value for the emission profile. In the Hunter region, the seed values were provided from airborne thermal images and the high degree of specification in this regard enabled the use of only one monitor. To a large extent the success of the Hunter Valley experiment was due to the author's detailed knowledge of spontaneous combustion in the region. This guided the placement of the monitor downwind of the sources within the predominately north-westerly flow regime of the Hunter Valley. A monitor located outside the major zone of influence would have seriously compromised the results for this region.

In the Bowen Basin a less sophisticated method was required to seed the model using only the knowledge of mine site staff. At this site the model capability was

enhanced through the use of a second monitor. The model was able to identify regions not originally identified by staff as containing significant self-heating.

Another important possibility is that sources of CO_2 apart from spontaneous combustion may contribute to the measured emissions. This is a concern at open-cut coal mines where many of the mining operations depend on diesel powered equipment. The greenhouse gas contribution from fuel at a number of open-cut mines was recently estimated by Day et al. (2010). They found that in the Hunter Valley fuel-derived emissions ranged from about 16 kt to 160 kt CO_2-e y^{-1}, depending on the size of the mine. Given the annual production of the Hunter Valley mines examined here it is probable that the contribution from diesel machinery would be less than 100 kt CO_2-e y^{-1}. For the Bowen Basin mine, about 30 kt CO_2-e y^{-1} is attributed to combustion of fuel on site. Although significant, fuel emissions represent only around 10 % of the emissions measured in this study. Nevertheless, it is possible that machinery operating near the fixed CO_2 monitors could result in high readings that would result in overestimating emissions from spontaneous combustion. However, the monitoring sites were selected as much as possible to avoid vehicle emissions and as an added precaution, the data were filtered to remove short-term disturbances caused by vehicles passing nearby. It should also be remembered that the thermal technique did not detect fuel emissions so given the convergence of the three methods, spontaneous combustion is probably the principal source of CO_2 emissions from the mine sites examined in this study.

5 Conclusions

In the current work three methods based on a) thermal infrared thermography b) plume traverses and c) inverse modelling methods have been used to estimate the emissions of CO_2 from spontaneous combustion in spoil piles. Each of the three methods has significant uncertainty illustrating the difficulty of obtaining quantitative values for this emission category. Nevertheless, within the large uncertainty, there is significant overlap of the three approaches indicating that this emission source requires further work in order to be quantified to the point where it can be included in national emissions inventories.

While the methods have been demonstrated to provide overall emission rates from spontaneous combustion over large areas, considerably further development is required in order to reduce the uncertainty to an acceptable level.

Acknowledgements

We would like to thank staff at the Bayswater power station and the Bowen Basin mine for their help in establishing monitor locations and providing meteorological data. In particular, the authors sincerely thank Claire Foley.

References

Australian Government Bureau of Meteorology (2010) Climate statistics for Australian locations. http://www.bom.gov.au/climate/averages/tables/cw_061275.shtml (accessed 3 August 2010).

Carras, J.N., Young, B.C., 1994. Self-heating of coal and related materials: Models, applications and test methods. Progress in Energy and Combustion Science 20, 1-15.

Carras, J.N., D., S.J., Saghafi, A., Williams, D.J. (2009) Greenhouse gas emissions from low-temperature oxidation and spontaneous combustion at open-cut coal mines in Australia. International Journal of Coal Geology 78, 161-168.

Day, S.J., Carras, Fry, R., Williams, D.J. (2010) Greenhouse gas emissions from Australian open-cut coal mines: contribution from spontaneous combustion and low-temperature oxidation. Environmental Monitoring and Assessment (in press) DOI 10.1007/s10661-009-1021-7.

Finkelman, R.B., 2004. Potential health impacts of burning coal beds and waste banks. International Journal of Coal Geology 59, 19-24.

Glasser, D., Bradshaw, S., 1990. in Handbook of Heat and Mass Transfer, (N.Cheremisinoff, Ed., Gulf, New Jersey), 4:1071.

Huang, C.H., 1979. A theory of dispersion in turbulent shear. Atmospheric Environment 13, 453-463.

Hurley, P.J., 2005. The Air Pollution Model (TAPM) Version 3. Part 1: Technical Description. CSIRO Atmospheric Research Technical Paper No. 71. CSIRO Marine and Atmospheric Research, Aspendale, VIC.

IPCC, 2007. 2006 IPCC guidelines for national greenhouse gas inventories (in five volumes), Prepared by the National Greenhouse Gas Inventories Programme, Eggleston, S., Buendia, L., Miwa, K., Ngara,T. and Tanabe, K. (Eds) Published IGES, Japan (available from http://www.ipcc-nggip.iges.or.jp/public/2006gl/index.htm).

Lehning M., Chang D.P.Y., Shonnard D.R., Bell, R.L., 1994. An inversion algorithm for determining area-source emissions from downwind concentration measurements. Journal of Air and Waste Management Association 44, 1204-1213.

Loh, Z., Leuning, R., Zegelin, S., Etheridge, D., Bai, M., Naylor, T., Griffith, D., 2009. Testing Lagrangian atmospheric dispersion modelling to monitor CO_2 and CH_4 leakage from geosequestration. Atmospheric Environment 43, 2602-2611.

Luhar, A.K., Hurley, P.J., 2003. Evaluation of TAPM, a prognostic meteorological and air pollution model, using urban and rural point-source data. Atmospheric Environment 37, 2795-2810.

Nelson, M.I., Chen, X.D., 2007. Survey of experimental work on the self heating and spontaneous combustion of coal, in Stracher, G.B., ed., Geology of coal fires: case studies from around the world. The Geological Society of America, 31-83.

Stracher, G.B., Taylor, T.P., 2004. Coal fires burning out of control around the world: thermodynamic recipe for environmental catastrophe. International Journal of Coal Geology 59, 7-17.

Walker, S., 1999. Uncontrolled fires in coal and coal wastes. IEA Coal Research, London. 72 pp.

Zawar-Reza, P., Kingham, S., Pearce, J., 2005. Evaluation of a year-long dispersion modelling of PM10 using the mesoscale model TAPM for Christchurch, New Zealand. Science of the Total Environment 349, 249-259.

Table 1. Emission flux estimates for the region studied in the Hunter Valley, New South Wales.

Method	Detail		Emission Flux		Averaging Timescale
			(kg CO_2-e s^{-1})	(kt CO_2-e y^{-1})	
Traverse	*Date*	*Time*			~ 30 minutes
	12/7/05	1730	51	1620	
	21/7/05	1230	26	815	
	23/8/05	1020	37	1180	
	23/8/05	1150	41	1290	
	6/12/05	1300	117	3690	
	6/12/05	1330	178	5610	
Thermography	*10 °C threshold temp)*		76	2400	< 10 minutes
Inverse modelling	*Stability Class E*		33	1040	6 months
	Stability Class D		50.7	1600	

Table 2. Emission flux estimates for the region studied in the Bowen Basin, Queensland.

Method	Detail	Emission Flux		Averaging Timescale
		(kg CO_2-e s^{-1})	(kt CO_2-e y^{-1})	
Inverse modelling	*Stability Class E*	6	200	3 months
	Stability Class D	10	320	

Figure Captions

Figure 1. The relationship between ground surface temperature and emissions flux (data from Carras et al., 2009).

Figure 2. Modelling domain for the Hunter Valley region.

Figure 3. Modelling domain for the Bowen Basin region.

Figure 4. Distribution of the area of ground in the Hunter Valley mines as a function of the ground temperature. The area of ground with temperatures below 10 °C have been excluded since emissions were assumed to be zero in these areas.

Figure 5. Example of plume traversing measurements made at the Hunter Valley site. The plots represent two consecutive runs; solid circle markers Traverse 1, open squares Traverse 2. The solid line indicates the route taken, which was approximately 5 km long.

Figure 6. Emission flux estimates from inverse modelling for the Hunter Valley site with atmospheric stability class D (a) and E (b). The flux estimate derived from the thermal imagery is also shown (c). The emission flux shown are expressed in units of g CO_2 s^{-1} per 50 m grid cell.

Figure 7. Emission flux estimates from inverse modelling for the Bowen Basin site with atmospheric stability class D (a) and E (b). The grid and estimates areas of emissions used to initialise the model is also shown (c). The emission flux shown are expressed in units of g CO_2 s^{-1} per 50 m grid cell.

Figure 8. The emission flux ranges estimated for the Hunter Valley for all three methods.

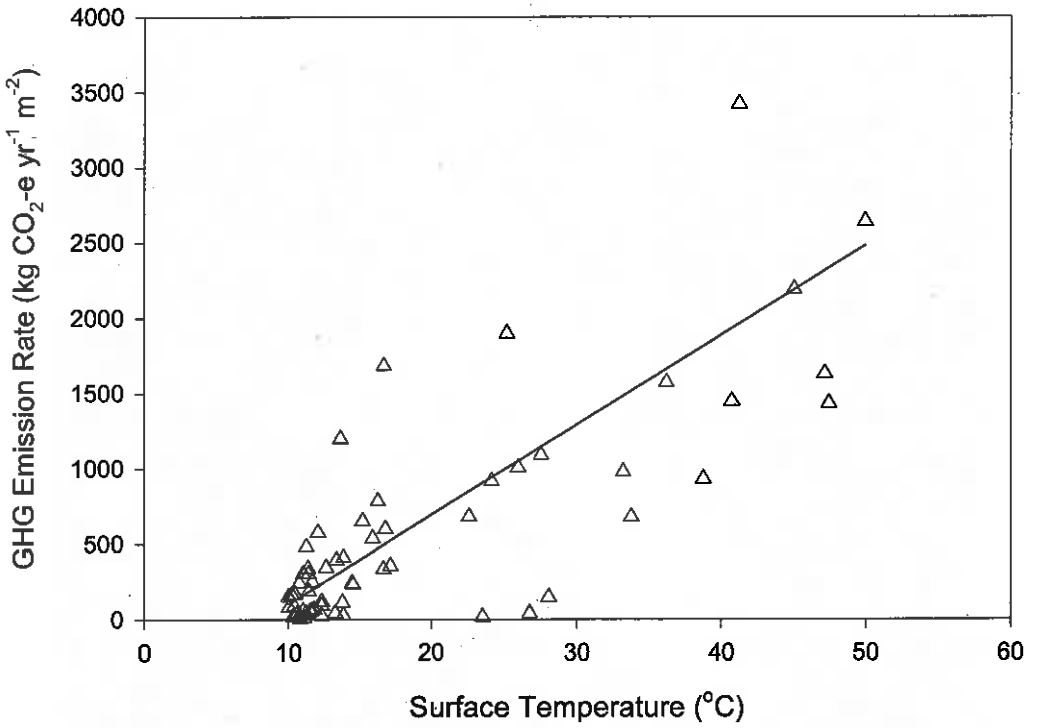
GHG Emission Rate (kg CO_2-e yr^{-1} m^{-2})
4000
3500
3000
2500
2000
1500
1000
500
0
0
10
20
30
40
50
60
Surface Temperature (°C)

Figure 1

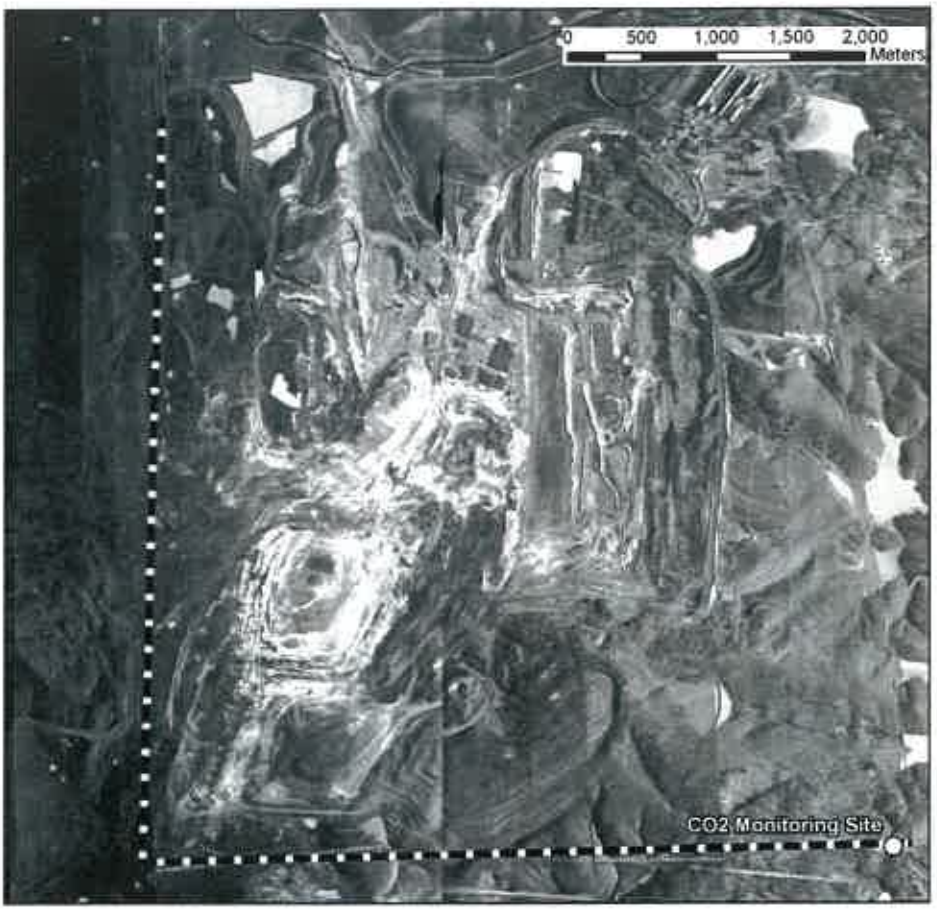

Figure 2


CO2 Monitoring Site 1
CO2 Monitoring Site 2
0
500
1,000
1,500
2,000
Meters

Figure 3

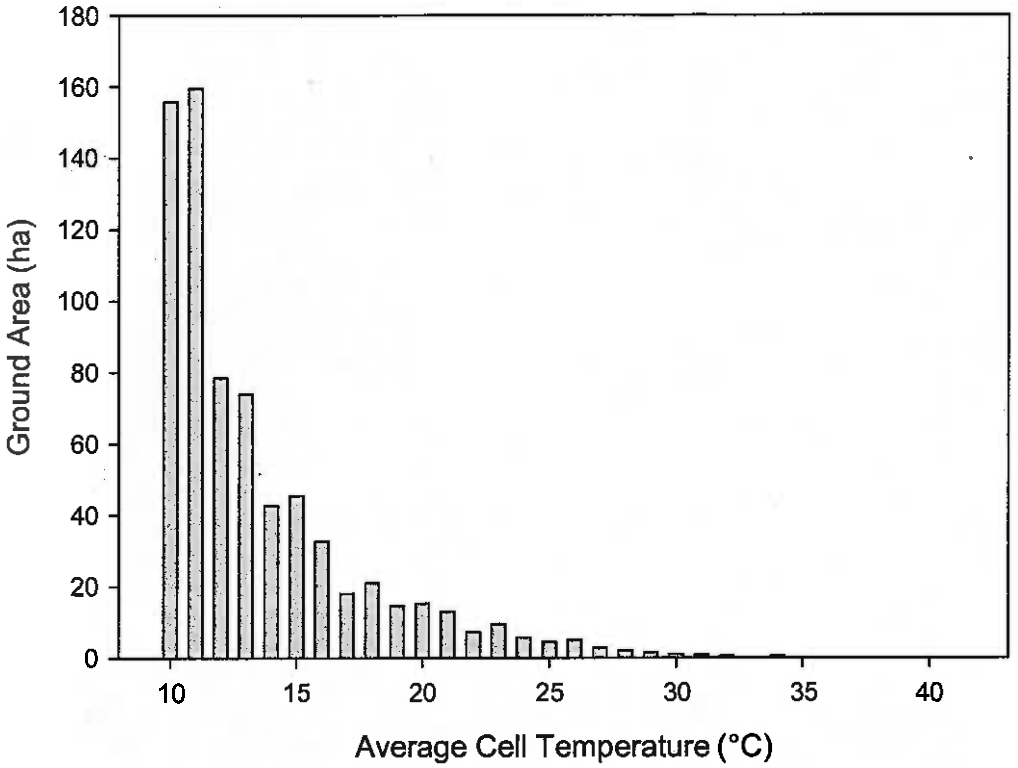
180
160
140
120
100
80
60
40
20
0
Ground Area (ha)
10
15
20
25
30
35
40
Average Cell Temperature (°C)

Figure 4

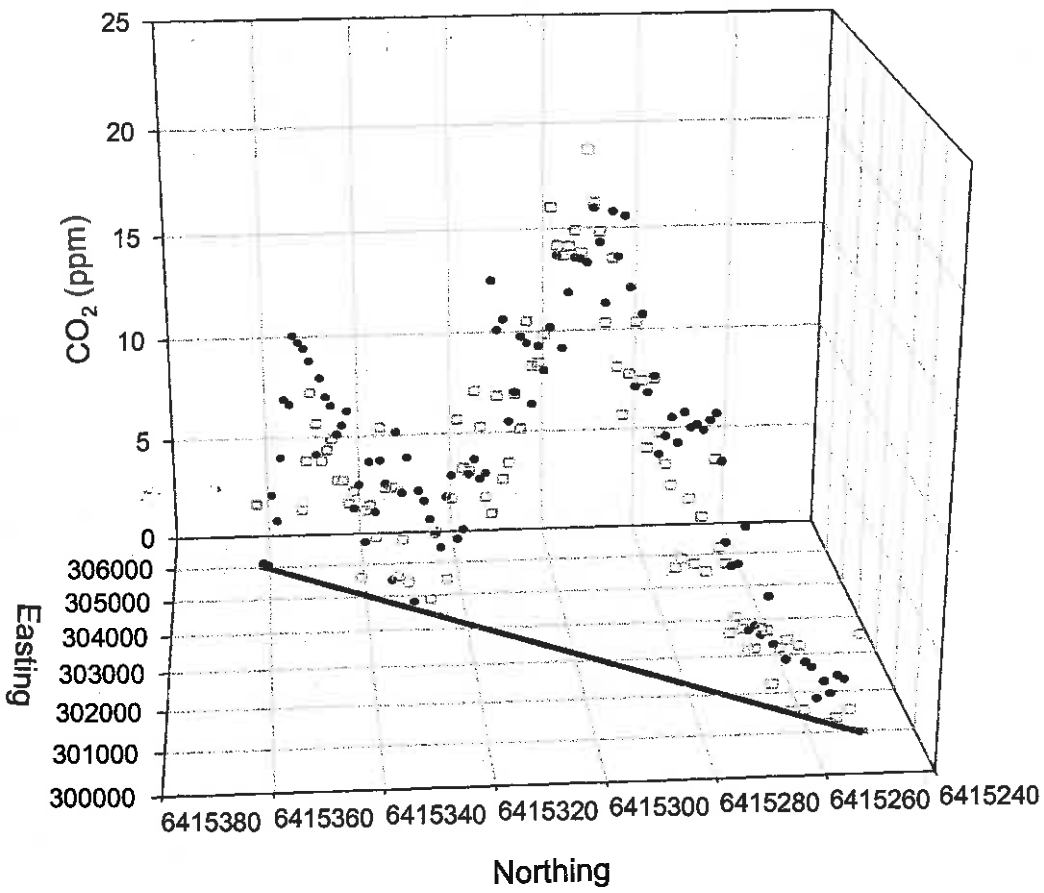
25
20
15
10
5
0
CO_2 (ppm)
306000
305000
304000
303000
302000
301000
300000
Easting
6415380 6415360 6415340 6415320 6415300 6415280 6415260 6415240
Northing

Figure 5

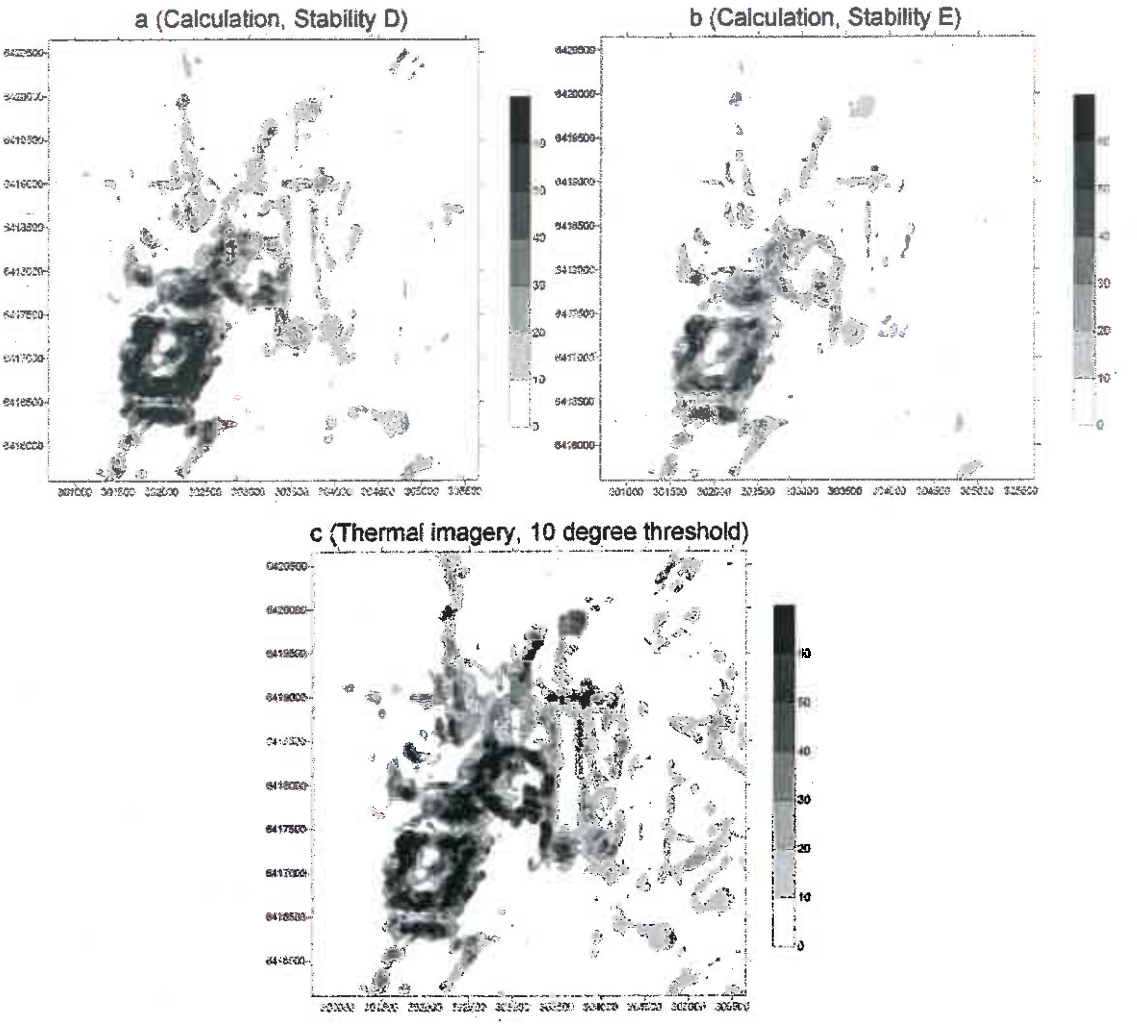
a (Calculation, Stability D)
b (Calculation, Stability E)
c (Thermal imagery, 10 degree threshold)

Figure 6

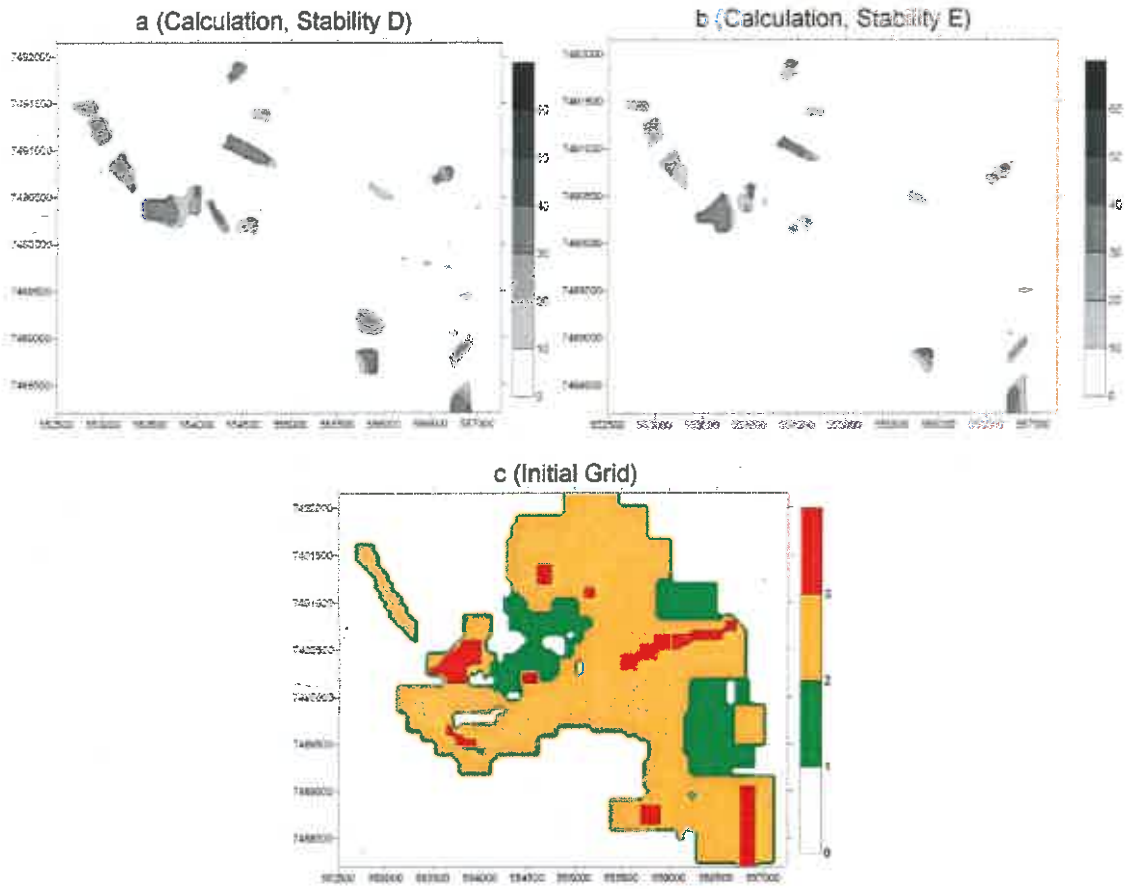
a (Calculation, Stability D)
b (Calculation, Stability E)
c (Initial Grid)

Figure 7

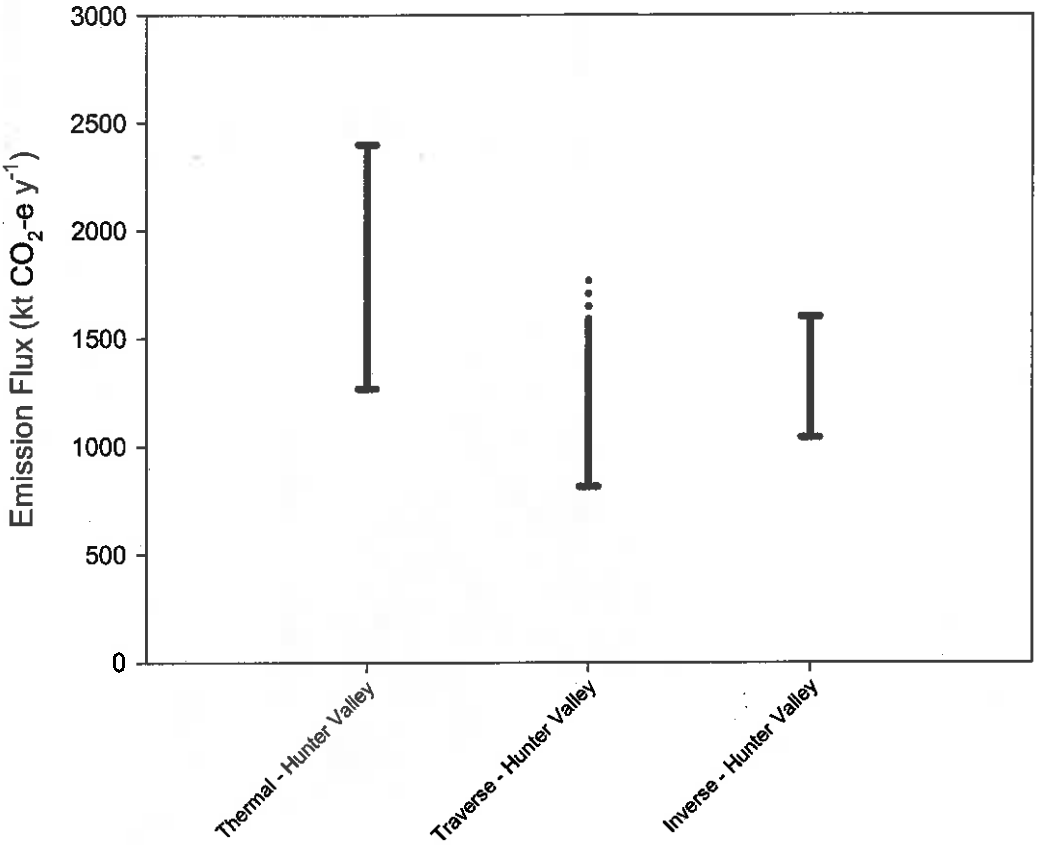
3000
2500
2000
1500
1000
500
0
Emission Flux (kt CO_2-e y^{-1})
Thermal - Hunter Valley
Traverse - Hunter Valley
Inverse - Hunter Valley

Figure 8